CCFE
CULHAM CENTRE FOR FUSION ENERGY

UK Atomic Energy Authority

UKAEA-CCFE-CP(20)113

J. Simpson, D. Moulton, C. Giroud, F. Casson, M. Groth, A. Chankin, L. Horvath, D. S. Gahle, F. Kochl

An examination of the Neutral penetration model 1/ne,ped scaling for its validity of spatially varying neutral sources

An examination of the Neutral penetration model 1/ne,ped scaling for its validity of spatially varying neutral sources

J. Simpson, D. Moulton, C. Giroud, F. Casson, M. Groth, A. Chankin, L. Horvath, D. S. Gahle, F. Kochl

This paper has been submitted to
24th International Conference on Plasma Surface Interactions in Controlled Fusion Devices (PSI), South Korea, 24 - 29 January 2021

An examination of the Neutral Penetration Model $1/n_{e,ped}$ scaling for its validity of spatially varying neutral sources

J. Simpson[1,2], D. Moulton[1] , C. Giroud[1], F. Casson[1],
M. Groth[2], A. Chankin[3], L. Horvath[1],
D. S. Gahle[4], L. Garzotti[1], G. Corrigan[1], F. Kochl[1] and JET contributors[5]

[1] CCFE, Culham Science Centre, Abingdon, OX14 3DB, UK
[2] Aalto University, FI-00076 AALTO, Espoo, Finland ,
[3] Max-Planck-Institut für Plasmaphysik, Boltzmannstraße 2,
D-85748 Garching,
[4] University of Strathclyde, 16 Richmond St, Glasgow G1 1XQ
[5]See the author list of E. Joffrin et al. accepted for publication in
Nuclear Fusion Special issue 2019,
https://doi.org/10.1088/1741-4326/ab2276

Abstract

EDGE2D-EIRENE simulations show that for a H-mode JET discharge (92168) the dominant atomic neutral deuterium source at the separatrix originates from the inner divertor target. Within JETTO-EIRENE neutral sources are placed at the X-point and outer midplane (OMP). For fixed electron and ion temperature, transport and neutral temperature it is observed that the $1/n_{e,ped}$ scaling (from reference the Neutral Penetration model (NPM) [1]) is observed when fueling at the OMP but not at the X-point. This is due to measuring the resultant density profiles at the OMP. When measuring the X-point fueling cases along the same coordinate which neutrals are injected along the $1/n_{e,ped}$ scaling is observed. Experimentally this scaling could be checked by remapping experimentally measure pedestal density profiles to a coordinate in the Z direction which intersects the X-point. Furthermore EUROPED [2] could accept a density profile defined on this coordinate system which would negate the need for a E factor, assuming that neutral source enters exclusively at the X-point.

1 Introduction

The core, Pedestal and SOL are interlinked, with conditions in one affecting the other. Stiff core profiles [3] mean an increase in the pedestal height causes an increase in the core profile which is optimal for fusion performance. The SOL provides boundary conditions to the pedestal which have also been shown to affect the MHD stability of the pedestal [4], [5].

The atomic neutral deuterium (from now on just referred to as 'neutrals') source from recycling at the divertor target is typically an order of magnitude greater than the gas puff [6], [7] (depending the divertor configuration and the gas puff position poloidally) in the high recycling regime in JET . This implies that the gas rate may potentially play a second order role in setting the density pedestal. Experimentally, it is unclear whether gas injection can effect the density pedestal or what indeed controls the density pedestal profile. However, it is clear that density pedestal is dependent on many other parameters, for example the divertor configuration, plasma current and triangularity [8] [9] [10] [11].

A model to predict the pedestal is critical to predict future performance. Models such as EPED [12], [13] attempt to predict the pressure pedestal assume the pedestal density height, $n_{e,ped}$ and width, Δ_{ne} as an input. The density profile is not always known *a priori* unless it can be controlled by engineering parameters such as gas injection rate, which as previously stated is not always the case.

The only analytic model (at least known to these authors) to predict the density pedestal is the neutral penetration model (NPM) [14]. The key prediction of the NPM is that the density pedestal width, Δ_{ne} , is proportional to $1/n_{e,ped}$. Experimental evidence however shows that predictions made by the NPM are not observed [8], [15], [16]. Modelling with BOUT, a fluid turbulence code, coupled with a simple analytic model for neutrals, showed a reduction in Δ_{ne} for increase $n_{e,ped}$ [17]. Modelling using the KN1D code (1D kinetic neutral code) showed no change in Δ_{ne} for an increase in $n_{e,ped}$ for C-mod but for DIII-D a change in Δ_{ne} was observed for increase in $n_{e,ped}$. Work by reference [16] showed that NPM is not valid when considering inter-ELM evolution. However, the NPM has been successfully used within the EUROPED code [2] which is similar to the EPED model but incorporates a model for the density pedestal prediction via the NPM (using the $1/n_{e,ped}$ scaling). Prediction by the EUROPED model are sensitive to the poloidal fueling profile characterised by the E factor, defined within the NPM, which accounts for the poloidal flux expansion between the measured (poloidal) position of the density profile, and the poloidal position of the dominant source of neutrals crossing the separatrix. Furthermore the E factor also has dependence on gas rate seen in equation 9 of reference [2]. The NPM implies that the position at which the dominant atomic neutral source crosses the separatrix is critical for pedestal predictions.

2 The neutral penetration model

An analytic way to calculate the density profile is the neutral penetration model (NPM) [1]. The NPM is based on a balance between the incoming atomic neutral flux, the ionisation source and diffusive electron particle transport. For simplicity we define the model along a coordinate x_{inj} which the neutrals are injected along (thus removing the E factor which is defined in reference [1]):

$$D_c \frac{d^2 n_e}{dx^2} = n_n(x_{inj}) n_e(x_{inj}) S_i \tag{1}$$

$$v_0 \frac{dn_n}{dx} = -n_n(x_{inj}) n_e(x_{inj}) S_i \tag{2}$$

where D_c is the core diffusion coefficient on closed flux surfaces, S_i is the ionisation source, n_n is neutral density, n_e is electron density and v_0 is the neutral velocity. The neutral source is assumed to originate only at separatrix at x_{inj}.

Equating equations 1 and 2 a second order differential equation can be derived, the solution to which is a *tanh* function. Once boundary conditions are applied an equation for the density profile can be derived:

$$n_e(x_{inj}) = n_{e,ped} tanh \left(tanh^{-1} \left[\frac{n_{e,sep}}{n_{e,ped}} \right] - \frac{S_i}{2v_0} n_{e,ped} x_{inj} \right), \tag{3}$$

where $n_{e,ped}$ is the density pedestal height (corresponding to the density at $x_{inj} \to -\infty$), $n_{e,sep}$ (corresponding to density at $x_{inj} = 0$) is the density at the separatrix. We point the reader to references [14] and [18] for more detailed derivation of equation 3 and details on the solution to differential equation (including equation 3) can be found in reference [19].

A key prediction from equation 3 is that assuming $tanh^{-1}(n_{e,sep}/n_{e,ped})$ is small compared to the other term, the characteristic distance to achieve $n_{e,ped}$ from the separatrix (Δ_{ne}) is then:

$$\Delta_{ne} = \frac{2v_0}{S_i n_{e,ped}} \tag{4}$$

This equation provides a simple analytic equation to calculate the pedestal width (Δ_{ne}) and provides the scaling $\Delta_{ne} \propto 1/n_{e,ped}$ which is measured along x_{inj}. This scaling is key for density pedestal predictions and will be examined later in the results section.

Typically the Δ_{ne} is given at the OMP, as experimentally this is where pedestal profiles are approximately measured in JET, but the neutral source may enter elsewhere (poloidally). To transform between the poloidal position at which the neutrals enter (x_{inj}), to a the poloidal position where the density profile is measured (x_m) is achieved by:

$$x_{inj} = x_m \cdot f(\theta_{inj}) / f(\theta_m), \tag{5}$$

where $f(\theta_{inj}) = dx_{inj}/d\psi$ and $f(\theta_m) = dx_m/d\psi$ where dx_{inj} is the local flux surface spacing along x_{inj} and dx_m is the local flux surface spacing along x_m

both given in he $\nabla\psi$ direction (i.e. perpendicular spacing). We define $E = f(\theta_{inj})/f(\theta_m)$ as per reference [1]. The physical motivation for $f(\theta)$ is to account for the increased real distance between flux surfaces at the neutral injection i.e. $f(\theta_{inj}$) position compared to the measurement position (i.e. $f(\theta_m)$). In this case $E = dx_{inj}/dx_m$ which represent the poloidal flux expansion. This results in equation 4 having the E factor in the denominator of Δ_{ne} is to be calculated at x_m.

Reference [1] assumes that E takes a scalar value and can only vary as function of poloidal angle and does not vary along x_{inj} however importantly it is found this is not the case (Fig. 1 - red line). The E factor varies significantly along x_{inj} especially over the region of strong ionisation, shown by the red dashed line Fig. 1 chosen for a point in the simulation neutral scan (X-point fueled case with the neutral influx equal to $31 \times 10^{21}\ s^{-1}$). This simple finding, that the poloidal flux expansion from X-point to OMP can vary significantly over the flux surfaces on which ionisation occurs, is an important result from this work. As will be shown below, it means that when neutrals are injected at the X-point, the $1/n_{e,ped}$ scaling predicted by the NPM can be satisfied along the injection coordinate, while at the same time being a poor match to profiles along the OMP coordinate.

In figure 1 the E factor is calculated using the EDGE2D [20] grid (which was used to set the boundary conditions for JETTO-EIRENE described in section 4) because the rows align with $\nabla\psi$ which is required to calculate the E factor.

3 JETTO-EIRENE simulations of a JET H-mode pedestal

A recent JET H-mode discharge (92168 at 44.62 s, 1.36 MA/1.9 T) operated in a tile 5 divertor configuration was chosen for this study as both the pedestal and core were well diagnosed and a well constrained EDGE2D-EIRENE [20] [21] [22] simulation was available, which was critical in setting the JETTO-EIRENE boundary conditions. The 1D transport code JETTO [23] was run in interpretive mode (i.e. fixed non-varying profiles) for the electron and ion temperature (T_e , T_i) and predictive mode for the electron density (n_e). A fixed diffusivity was used for the particle transport $D_\perp = 0.05\, m^2 s^{-1}$ taken from the EDGE2D-EIRENE simulation in the pedestal region. The JETTO separatrix boundary conditions were taken from aforementioned EDGE2D-EIRENE simulation. The separatrix boundary conditions were as follows: electron density ($1.68 \times 10^{19}\, m^{-3}$) , electron temperature ($116\ eV$) and ion temperature ($480\ eV$). Note for the presented simulations $tanh^{-1}(n_{e,sep}/n_{e,ped}) << 1$ which is consistent with the assumptions needed to derive equation 4. The EIRENE kinetic neutral model [21] requires the integrated neutral influx at the separatrix ($7.75 \times 10^{21} s^{-1}$) and the average neutral energy on the separatrix ($156\ eV$) which were also taken from the previously stated EDGE2D-EIRENE simulation.

The variation of the density profile as calculated by JETTO-EIRENE were

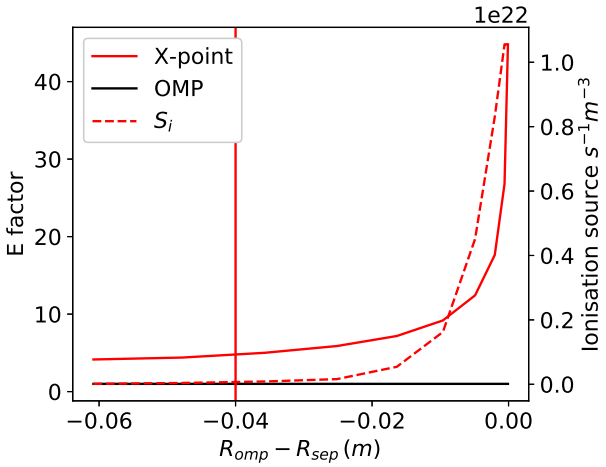

Figure 1: Poloidal flux expansion factor E (defined in section 2) as a function of radial distance at the outer midplane. The coloured solid lines show the E factor calculated at different poloidal locations as per the legend. The outer midplane is the reference viewing location thus E=1. The dashed red line is the ionisation source for X-point fueled case with neutral injection rate equal to $31 \times 10^{21}\ s^{-1}$ and the pedestal width for this case is plotted as the vertical red line.

studied for a static equilibrium (taken from EFIT at 44.62s) when the neutral source is varied for a fixed particle diffusion and temperature profiles. In this setup only a change in the ionisation source driven by cold neutrals (i.e. equal to 156 eV) and/or hot (charged exchanged) neutrals can affect the density profile. The position of the neutral source is set at the separatrix either at the OMP or X-point (fig. 2 red and black lines), such that the source is always approximately perpendicular to the flux surfaces (at the separatrix). The initial velocity vector / injection coordinate, x_{inj} , is either the red line in Fig. 2 for the OMP fueling or the black line in Fig. 2 for the X-point fueling. It should be noted that the black (solid) line in Fig. 2 does not follow $\nabla\psi$. Although EIRENE is 3D, toroidal symmetry is assumed. Furthermore since JETTO is a 1D code and so any poloidal asymmetry in the neutral source is translated into a flux surface average to calculate the ionisation source and thus the density profile, which is given as a function of OMP real coordinate. In the initial simulations unless otherwise stated charge exchange is turned off and the ionisation rate coefficient for deuterium comes from HYDHEL database (Eq. H.2 2.1.5, in reference [24]). Note that the effective ionisation rate usually used in EIRENE is dependent also on the local electron density, however, this dependence is very weak (see figure 6 [25]). For all simulations the neutral recombination process in EIRENE is turned off.

4 Results

4.1 EDGE2D prediction of neutral fluxes at the separatrix

EDGE2D-EIRENE shows that the dominant source of neutrals which reaches the separatrix comes from the inner target (Fig. 3) for the discharge in question (92168 outlined in section 3), which is consistent with the analysis from reference [6]. Activating only specific neutral sources in EIRENE, the inner target, outer target or neutral gas puff, and then evolving EIRENE for one time step, allowed the observation of which source provides the most neutral flux across the separatrix.

4.2 Predicted JETTO-EIRENE pedestals

Pedestal heights and widths were extracted from the density profiles calculated by JETTO-EIRENE using a modified tanh (mtanh) fitting method [26].

Equation 1 in reference [26] is fitted to the JETTO-EIRENE density profile. Note JETTO-EIRENE provides no information about the SOL. Within equation 1 [26] the parameter a_{sol} can potentially take two different values, 0 implying density goes to zero outside of the SOL or -$n_{e,ped}$ due to the definition of equation 3. As such all figures containing $n_{e,ped}$ and Δ_{ne} will be plotted with an error bar such that the limits of these error bars show the calculated $n_{e,ped}$ and Δ_{ne} for each choice of a_{sol}. The proceeding figures will also show the average between $a_{sol} = 0$ & - $n_{e,ped}$ for Δ_{ne} and $n_{e,ped}$ which will be shown as a

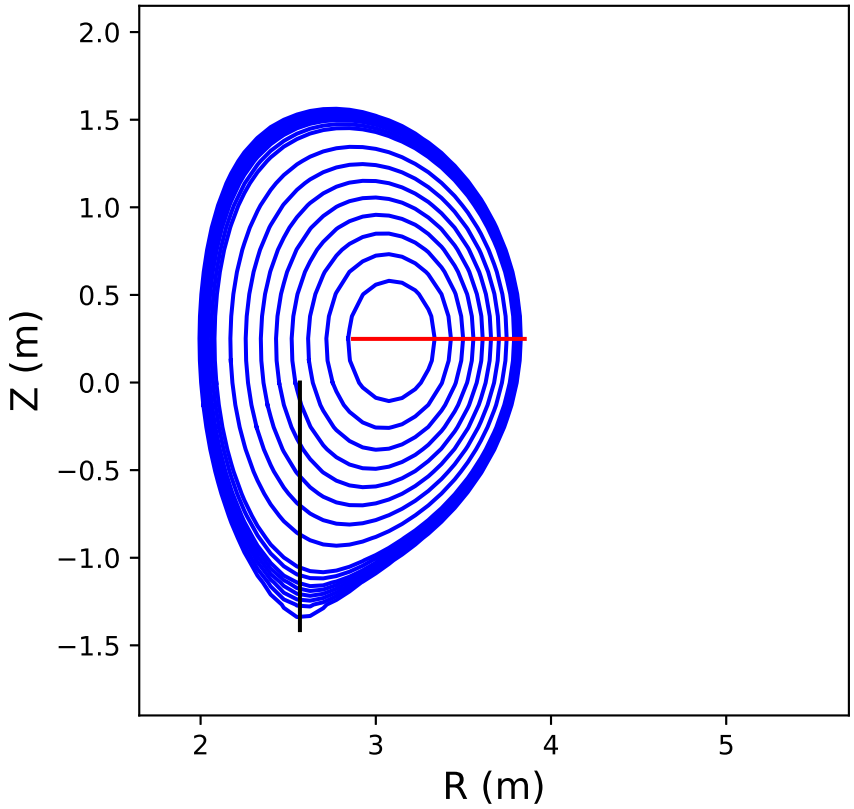

Figure 2: Equilibrium used for the JETTO-EIRENE simulations denoting the injection location of the point source of neutrals (on the separatrix) at the outer midplane (red) and X-point (black). The extent of the line demonstrates the direction of the inital velocity vector of the neutrals.

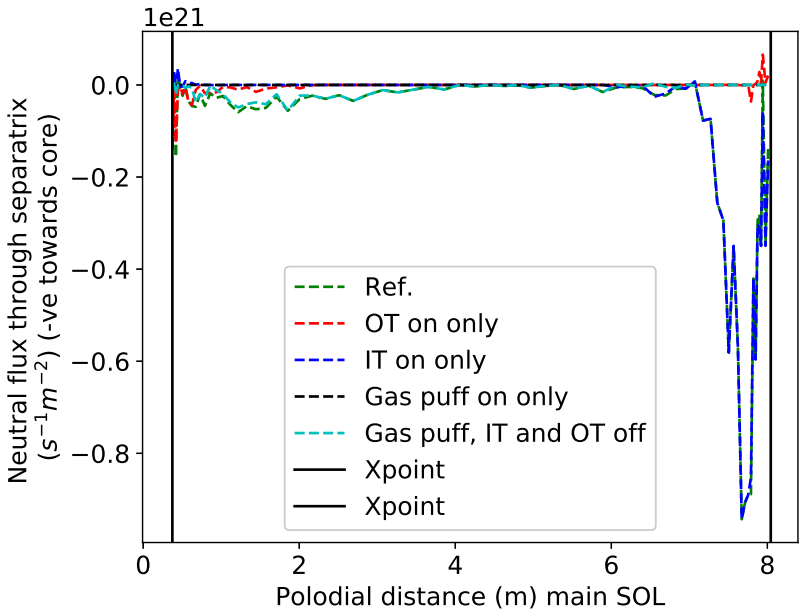

Figure 3: Neutral source at individual poloidal locations along the separatrix. Each line shows the neutral particle flux density crossing the separatrix (as a function poloidal location) which originate from a particular neutral source. Blue line - inner target, red line - outer target and the green line is the sum off all neutral sources. Note that negative direction is towards the core. The extremes of the x axis are located in real space adjacent to each other and show the X-point shown by the vertical black lines.

marker. This average $n_{e,ped}$ & Δ_{ne} will be used to calculate normalised χ^2 fits of the $1/n_{e,ped}$ scaling. For the presented mtanh fits (to the density profiles) the normalised χ^2 ranged from 2×10^{-4} to 0.01 with an average of 3×10^{-3} .

Equation 3 and equation 1 in reference [26] have different definitions of the pedestal width, Δ_{ne} . For a correct comparison Δ_{ne} from the mtanh fit should be compared to the $2{\cdot}\Delta_{ne}$ from equation 4.

4.3 Pedestal scaling assuming x_{inj} along the OMP

When the neutral source is placed at the OMP it is observed for a neutral source scan from 7.75×10^{21} to 93×10^{21} (increasing in factors of two) particles per second that the $1/n_{e,ped}$ scaling is followed - star markers on figure 4a and the fitted red dotted line (which has very small χ^2). This result was to be expected as the simulation were set up to satisfy all the NPM assumptions: flat electron temperature profile (in this case = 800 eV) so that the effective ionisation rate is constant (as it is only dependent on electron temperature), charge exchange process is turned off in EIRENE and the profile is measured along x_{inj} at the OMP where the neutral source is also placed (i.e E=1). Therefore similar agreement with equation 3 was found. The inputs to equation 3 were as follows: ionisation cross section at 800 eV, E=1, $n_{e,ped}$ = density value in the core, $n_{e,sep} = 1.68 \times 10^{21}$ and $v_0 = \sqrt{2kT/m}$ where T=156 eV, k is the Boltzman constant and m is the mass of a atomic deuterium. Furthermore, if Δ_{ne} from the tanh fit was compared to the $2{\cdot}\Delta_{ne}$ from equation 4 they too would also be equal.

Assuming the experimental electron and ion temperature profiles from 92168 and CX is turned on the $1/n_{e,ped}$ scaling is still observed (square markers Fig. 4a and black dotted line which also has a small χ^2 value).

The same analysis was done for the neutral source at the X-point (x_{inj} along the black line in Fig. 2) instead of the OMP. The profiles are measured (x_m) at the OMP. For both the flat and experimental temperature profiles cases, the $1/n_{e,ped}$ scaling is not recovered when measuring along the OMP coordinate, x_m (Fig. 4b, χ^2 is large for the $1/n_{e,ped}$ fits). Note also the drop in $n_{e,ped}$ when fueling at the X-point compared to the OMP (comparable markers and colours Fig. 4a & Fig. 4b)

4.4 Pedestal scaling assuming x_{inj} along the X-point

The $1/n_{e,ped}$ scaling is observed when fueling at the X-point when the profile is measured along x_{inj} at the X-point (Fig. 5). However it is not recovered when measured along the OMP (red dashed line Fig. 2 which has very large χ^2 value). Both sets of simulations using either flat temperature profile or experimental temperature profiles now follow the $1/n_{e,ped}$ scaling. The χ^2 of the $1/n_{e,ped}$ fits reduce significantly for comparable lines in figure 4b and fig. 5. To capture the radial variation in the spacing between flux surfaces Δ_{ne} and $n_{e,ped}$ were re-calculated using the x-axis of the mtanh along x_{inj} at the X-point given by the by black line in Fig. 2.

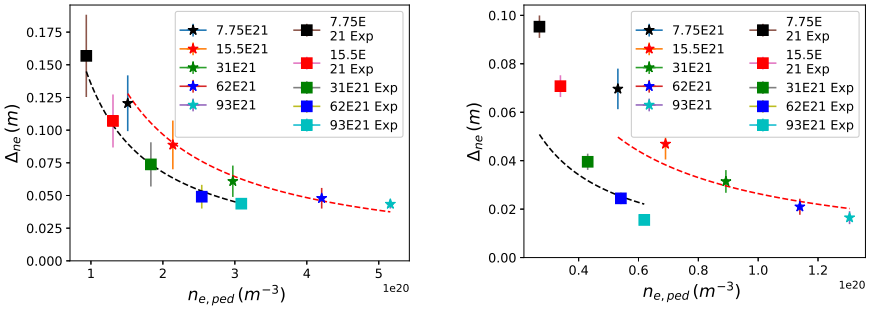

(a) Red dashed line $\chi^2 = 0.005$
Black dashed line $\chi^2 = 0.002$

(b) Red dashed line $\chi^2 = 0.036$
Black dashed line $\chi^2 = 0.12$

Figure 4: A neutral source scan where the neutral source is placed either at the (a) outer midplane or (b) X-point. Δ_{ne} and $n_{e,ped}$ are calculated using a modified tanh (mtanh) fit [26]. The x-axis for the mtanh fit [26] is taken to be the coordinate at the OMP (red line in figure 2). The stars represent a simulation set up with a flat temperature profile and charge exchange (CX) turned off and the squares using the experimental temperature profiles and CX turned on. The dashed lines are the $1/n_{e,ped}$ scaling fitted using a normalised χ^2 fit. The neutral source scan shown here ranges from 7.75×10^{21} to 93×10^{21} particles per second as shown on the legend of the plot denoted by changing colour. The error bars extremes show different fitted $n_{e,ped}$ and Δ_{ne} for different offset parameters - $a_{sol} = 0$ & $-n_{e,ped}$ for equation (1) in reference [26]. The markers are an average between these two cases.

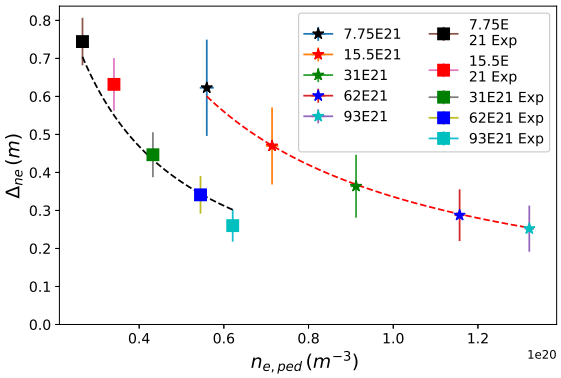

Figure 5: A neutral source scan where the neutral source is placed at the X-point. Δ_{ne} and $n_{e,ped}$ are calculated using a modified tanh (mtanh) fit [26]. The x-axis for the mtanh fit [26] is taken to be the coordinate at the X-point which neutral source is injected along (black line in figure 2). The stars represent a simulation set up with a flat temperature profile and charge exchange (CX) turned off and the squares using the experimental temperature profiles and CX turned on. The dashed lines are the $1/n_{e,ped}$ scaling fitted using a normalised χ^2 . $\chi^2 = 3\times10^{-4}$ for the red dashed line and $\chi^2 = 0.009$ for the black dashed line. Neutral source scan shown here ranges from 7.75×10^{21} to 93×10^{21} particles per second as shown on the legend of the plot denoted by changing colour. The error bar extremes show different fitted $n_{e,ped}$ and Δ_{ne} for different offset parameters - $a_{sol} = 0$ & -$n_{e,ped}$ for equation (1) in reference [26]. The markers are an average between these two cases.

The results from figures 4a and 4b would point to the conclusion that having the neutral source at the X-point and measuring it at the OMP is the reason why the $1/n_{e,ped}$ scaling is not observed. The NPM states that the $1/n_{e,ped}$ scaling should be predicted when neutral source and measurement position are in the same location (i.e. both are along x_{inj}). If measuring elsewhere (i.e. at different poloidal angles) an E factor needs to be considered, which the NPM assumes to be scalar. However it is already been shown (Fig. 1) that E is a function of x_{inj} and provided, E varies over the order of Δ_{ne} .

5 Discussion

This work only addresses part of the problem of a density pedestal prediction model - for a fixed temperature, transport profiles and neutral velocity, allowing only the density to vary in response to ionisation and CX from a separatrix point sources of atomic neutrals. In reality the neutral source is poloidally distributed at the separatrix (Fig. 3) which could effect the density pedestal.

It is likely that the neutral source, transport [27] and stability are all coupled, all having the ability to affect each other. The importance of each process is not yet fully understood. Ideally testing with EUROPED and a coupling to a pedestal transport model would ultimately be needed to confirm whether the $1/n_{e,ped}$ scaling is followed in more realistic cases.

Within this analysis CX has been discounted as potential mechanism for affecting the density profile. However it should be noted that CX in the SOL/divertor and fast reflection at the divertor targets could play a role in setting the density profile [28]. This analysis has only examined CX within the confined plasma and such cannot capture CX or fast reflection from outside the separatrix.

To derive equation 4 and hence the $1/n_{e,ped}$ scaling the term $tanh^{-1}(n_{e,sep}/n_{e,ped})$ has to be ignore in equation 3. Within the present simulation set $tanh^{-1}(n_{e,sep}/n_{e,ped}) << 1$. Simulations have been conducted where $tanh^{-1}(n_{e,sep}/n_{e,ped}) \approx \mathcal{O}(1)$. However they were not conducted over a large enough range of $n_{e,ped}$ to conclude whether the $1/n_{e,ped}$ scaling was observed, as such future work should address this point.

5.1 Potential improvements of the NPM

Moving the neutral source from the OMP to the X-point is the single cause of the disagreement of the prediction of the $1/n_{e,ped}$ scaling from the NPM (Figs. 4a and 4b) when measuring $n_{e,ped}$ and Δ_{ne} at the OMP. Fig. 5 shows for an X-point neutral source, that when the density profiles are remapped from the OMP coordinate (red line Fig. 2) to x_{inj} at the X-point (black line Fig. 2) and used for the mtanh fitting, the $1/n_{e,ped}$ scaling is observed, because E(x_{inj}) is accounted for.

Assuming the transport and temperature profiles are fixed, and that the dominant neutral source is a point source at the X-point, experimentally measured pedestal profiles (e.g. from a gas scan experiment) could be remapped to the X-point and the $1/n_{e,ped}$ scaling checked. If experimentally verified, EUROPED [2] could accept a pedestal pressure profile along a X-point coordinate (e.g. black line in Fig. 2) rather than the standard OMP coordinate. This then would negate the need to have an E factor in equation 4 which EUROPED uses to calculate $n_{e,ped}$ based off a fixed Δ_{ne} because $x_{inj} = x_m$. This is based on the assumption that the all of the neutral source enters at the X-point (i.e. the black line on figure 2), the density is a flux surface quantity and indeed the ionisation source is the driving factor in changing the density pedestal.

The E factor is found to be radially varying at the X-point (Fig. 1). The NPM assumes the majority of neutral source enters at one poloidal location which can be characterised by a scalar E factor. In reality it is likely the poloidal source enters over some poloidal angle and neutrals do not move perpendicular to flux surfaces. This could be one potential explanation as to why $1/n_{e,ped}$ scaling may not be observed experimentally (even when remapping to the X-point).

6 Conclusion

EDGE2D simulations show that the majority of the atomic neutrals which cross the separatrix originate from the inner divertor target for the particular JET case considered, low density H-mode plasma (horizontal divertor configuration, 1.3 MA). This motivated the consideration of the neutral source at the X-point in JETTO-EIRENE (Fig. 3) . A neutral source scan in JETTO-EIRENE demonstrates that fueling at the X-point breaks the $1/n_{e,ped}$ scaling when the resultant density profile is observed at the OMP (Fig. 4b). The $1/n_{e,ped}$ scaling can be recovered for the X-point fueling cases when remapping the density profiles from the OMP to the X-point (red to black lines in Fig. 2) because the coordinate at which the neutral are injected along is now the same as the mtanh fitting x axis (Fig. 5), i.e. $x_{inj} = x_m$. Hence when fueling at the OMP and observing the resultant density profile at the OMP the $1/n_{e,ped}$ scaling is observed (Fig. 4a). The same being true for fueling at the X-point that the $1/n_{e,ped}$ scaling is observed when measuring the resultant density profile along the coordinate which the neutrals are injected (i.e. along the X-point black line Fig 2).

Assuming that the temperature, transport and neutral velocity are fixed and that neutral source enters only at the X-point the observed $1/n_{e,ped}$ scaling could be experimentally observed. This can be achieved by remapping a experimental gas scan to the X-point. Furthermore, density profiles could be provided to SOL-pedestal integrated models , such as EUROPED, using a coordinate intersecting the X-point line (i.e. black line in Fig. 2). This would negate the need for an E factor, assuming that the dominant neutral source for the pedestal enters at the X-point (i.e. the source moves along the injection coordinate) and is responsible for setting the density pedestal.

Future work would need to relax the static temperature and transport profiles, to examine their impact on the $1/n_{e,ped}$ scaling. Such an endeavour would use an EPED like scaling [12] and/or MHD pedestal stability and a pedestal transport model. Furthermore it would provide insight into which process (transport, neutral source or stability) has the dominant effect on setting the density pedestal.

6.1 Acknowledgments

I would like to thank Alex Chankin for providing the EDGE2D-EIRENE simulation of the JET discharge 92168 which was integral in setting the boundary conditions for the JETTO-EIRENE simulations.

This work has been carried out within the framework of the EUROfusion Consortium and has received funding from the Euratom research and training programme 2014-2018 and 2019-2020 under grant agreement No 633053. The views and opinions expressed herein do not necessarily reflect those of the European Commission.

References

[1] R. J. Groebner, M. A. Mahdavi, A. W. Leonard, T. H. Osborne, G. D. Porter, R. J. Colchin, and L. W. Owen, "The role of neutrals in high-mode (H-mode) pedestal formation", *Physics of Plasmas*, vol. 9, no. 5, pp. 2134–2140, 2002, ISSN: 1070664X. DOI: 10.1063/1.1462032.

[2] S. Saarelma, C. D. Challis, L. Garzotti, L. Frassinetti, C. F. Maggi, M. Romanelli, and C. Stokes, "Integrated modelling of H-mode pedestal and confinement in JET-ILW", *Plasma Physics and Controlled Fusion*, vol. 60, no. 1, 2018, ISSN: 13616587. DOI: 10.1088/1361-6587/aa8d45.

[3] X. Garbet, P. Mantica, F. Ryter, G. Cordey, F. Imbeaux, C. Sozzi, A. Manini, E. Asp, V. Parail, and R. Wolf, "Profile stiffness and global confinement", *Plasma Physics and Controlled Fusion*, vol. 46, no. 9, pp. 1351–1373, 2004, ISSN: 07413335. DOI: 10.1088/0741-3335/46/9/002.

[4] S. Saarelma, a. Järvinen, M. Beurskens, C. Challis, L. Frassinetti, C. Giroud, M. Groth, M. Leyland, C. Maggi, and J. Simpson, "The effects of impurities and core pressure on pedestal stability in Joint European Torus (JET)a)", *Physics of Plasmas*, vol. 22, no. 5, p. 056 115, 2015, ISSN: 1070-664X. DOI: 10.1063/1.4921413. [Online]. Available: http://scitation.aip.org/content/aip/journal/pop/22/5/10.1063/1.4921413.

[5] J. Simpson, D. Moulton, C. Giroud, M. Groth, and G. Corrigan, "Using EDGE2D-EIRENE to simulate the effect of impurity seeding and fueling on the upstream electron separatrix temperature", *Nuclear Materials and Energy*, vol. 20, no. June, p. 100 599, 2019, ISSN: 23521791. DOI: 10.1016/j.nme.2019.02.002. [Online]. Available: https://doi.org/10.1016/j.nme.2019.02.002.

[6] M. Groth, G. D. Porter, T. D. Rognlien, S. Wiesen, M. Wischmeier, M. N. Beurskens, X. Bonnin, B. D. Bray, S. Brezinsek, N. H. Brooks, D. P. Coster, T. Eich, M. E. Fenstermacher, C. Fuchs, R. A. Groebner, D. Harting, A. Huber, S. Jachmich, A. Kallenbach, C. J. Lasnier, A. W. Leonard, A. Meigs, H. W. Müller, M. E. Rensink, D. L. Rudakov, J. G. Watkins, and E. Wolfrum, "Poloidal distribution of recycling sources and core plasma fueling in DIII-D, ASDEX-Upgrade and JET L-mode plasmas", *Plasma Physics and Controlled Fusion*, vol. 53, no. 12, 2011, ISSN: 07413335. DOI: 10.1088/0741-3335/53/12/124017.

[7] L. W. Owen, R. J. Colchin, R. Maingi, M. E. Fenstermacher, T. N. Carlstrom, and R. J. Groebner, "Origins and spatial distributions of core fueling in the DIII-D tokamak", *Journal of Nuclear Materials*, vol. 290-293, pp. 464–468, Mar. 2001, ISSN: 00223115. DOI: 10.1016/S0022-3115(00)00582-1.

[8] C. F. Maggi, L. Frassinetti, L. Horvath, A. Lunniss, S. Saarelma, H. Wilson, J. Flanagan, M. Leyland, I. Lupelli, S. Pamela, H. Urano, L. Garzotti, E. Lerche, I. Nunes, and F. Rimini, "Studies of the pedestal structure and inter-ELM pedestal evolution in JET with the ITER-like wall", *Nuclear*

Fusion, vol. 57, no. 11, aa7e8e, 2017, ISSN: 17414326. DOI: 10.1088/1741-4326/aa7e8e. [Online]. Available: https://doi.org/10.1088/1741-4326/aa7e8e.

[9] E. D. Luna, F. Rimini, P. Lomas, A. C. C. Sips, L. Frassinetti, and P. Drewelow, "Recent Results on High-Triangularity H-mode Studies in JET-ILW", pp. 1–8, 2014.

[10] C. Giroud, S. Jachmich, P. Jacquet, A. Jï¿rvinen, E. Lerche, F. Rimini, L. Aho-Mantila, N. Aiba, I. Balboa, P. Belo, C. Angioni, M. Beurskens, S. Brezinsek, F. J. Casson, I. Coffey, G. Cunningham, E. Delabie, S. Devaux, P. Drewelow, L. Frassinetti, A. Figueiredo, A. Huber, J. Hillesheim, L. Garzotti, M. Goniche, M. Groth, H. T. Kim, M. Leyland, P. Lomas, G. Maddison, S. Marsen, G. Matthews, A. Meigs, S. Menmuir, T. Puetterich, G. Van Rooij, S. Saarelma, M. Stamp, H. Urano, and A. Webster, "Progress at JET in integrating ITER-relevant core and edge plasmas within the constraints of an ITER-like wall", *Plasma Physics and Controlled Fusion*, vol. 57, no. 3, 2015, ISSN: 13616587. DOI: 10.1088/0741-3335/57/3/035004.

[11] J. W. Hughes, B. Labombard, J. Terry, A. Hubbard, and B. Lipschultz, "Edge profile stiffness and insensitivity of the density pedestal to neutral fuelling in Alcator C-Mod edge transport barriers", *Nuclear Fusion*, vol. 47, no. 8, pp. 1057–1063, Aug. 2007, ISSN: 00295515. DOI: 10.1088/0029-5515/47/8/041. [Online]. Available: https://iopscience.iop.org/article/10.1088/0029-5515/47/8/041%20https://iopscience.iop.org/article/10.1088/0029-5515/47/8/041/meta.

[12] P. B. Snyder, R. J. Groebner, A. W. Leonard, T. H. Osborne, and H. R. Wilson, "Development and validation of a predictive model for the pedestal height", *Physics of Plasmas*, vol. 16, no. 5, 2009, ISSN: 1070664X. DOI: 10.1063/1.3122146.

[13] P. Snyder, "A first-principles predictive model of the pedestal height and width: development, testing and ITER optimization with the EPED model Related content", *Nuclear Fusion*, vol. 51, no. 10, p. 103 016, Aug. 2011. DOI: 10.1088/0029-5515/51/10/103016. [Online]. Available: https://iopscience.iop.org/article/10.1088/0029-5515/51/10/103016%20https://iopscience.iop.org/article/10.1088/0029-5515/51/10/103016/meta.

[14] R. J. Groebner, M. A. Mahdavi, A. W. Leonard, T. H. Osborne, N. S. Wolf, G. D. Porter, P. C. Stangeby, N. S. Brooks, R. J. Colchin, and L. W. Owen, "Comparison of H-mode barrier width with a model of neutral penetration length", *Nuclear Fusion*, vol. 44, no. 1, pp. 204–213, 2004, ISSN: 00295515. DOI: 10.1088/0029-5515/44/1/022.

[15] J. W. Hughes, B. LaBombard, D. A. Mossessian, A. E. Hubbard, J. Terry, and T. Biewer, "Advances in measurement and modeling of the high-confinement-mode pedestal on the Alcator C-Mod tokamak", in *Physics of Plasmas*, vol. 13, American Institute of PhysicsAIP, May 2006, p. 056 103.

DOI: 10.1063/1.2180748. [Online]. Available: http://aip.scitation.org/doi/10.1063/1.2180748.

[16] R. Groebner, "Progress towards a predictive model for pedestal height in DIII-D Related content Temporal evolution of H-mode pedestal in DIII-D-Limits to the H-mode pedestal pressure gradient in DIII-D", 2009. DOI: 10.1088/0029-5515/49/8/085037.

[17] X. Q. Xu, W. M. Nevins, R. H. Cohen, T. D. Rognlien, and M. V. Umansky, "Correlation of density pedestal width and neutral penetration length", *Contributions to Plasma Physics*, vol. 44, no. 1-3, pp. 105–110, 2004, ISSN: 08631042. DOI: 10.1002/ctpp.200410015.

[18] M. A. Mahdavi, R. Maingi, R. J. Groebner, A. W. Leonard, T. H. Osborne, and G. Porter, "Physics of pedestal density profile formation and its impact on H-mode density limit in burning plasmas", *Physics of Plasmas*, vol. 10, no. 10, pp. 3984–3991, 2003, ISSN: 1070664X. DOI: 10.1063/1.1605101.

[19] *Physics of Plasma-Wall Interactions in Controlled Fusion*. 1986, ISBN: 9781475700695. DOI: 10.1007/978-1-4757-0067-1.

[20] R. Simonini, G. Corrigan, G. Radford, J. Spence, and A. Taroni, "Models and Numerics in the Multi-Fluid 2-D Edge Plasma Code EDGE2D/U", *Contributions to Plasma Physics*, vol. 34, no. 2-3, pp. 368–373, Jan. 1994, ISSN: 08631042. DOI: 10.1002/ctpp.2150340242. [Online]. Available: http://doi.wiley.com/10.1002/ctpp.2150340242.

[21] D. Reiter, "Progress in two-dimensional plasma edge modelling", *Jornual of Nuclear Material*, vol. 471, p. 196, 1992.

[22] C. Giroud, "To be submitted", *IAEA*, 2018.

[23] M. Romanelli, G. Corrigan, V. Parail, S. Wiesen, R. Ambrosino, and P. D. Silva Aresta Belo, "Luca GARZOTTI 1) , Derek HARTING 1) , Florian KÖCHL 1,5) , Tuomas KOSKELA 1,6)", *Elina MILITELLO-ASP*, vol. 9, no. 8, 2014. DOI: 10.1585/pfr.9.3403023.

[24] D. Reiter, "The data file HYDHEL : Atomic and Molecular Data for EIRENE based upon : Janev , Langer , Evans , Post , " Elementary Processes in Hydrogen-Helium Plasmas ", Springer 1987 FZ , Forschungszentrum J ulich GmbH FRG Available via E-mail from d.reiter@fz-jueli", pp. 1–216, 1987.

[25] P. C. Stangeby, "Basic physical processes and reduced models for plasma detachment", *Plasma Physics and Controlled Fusion*, vol. 60, no. 4, p. 44 022, 2018, ISSN: 13616587. DOI: 10.1088/1361-6587/aaacf6. [Online]. Available: http://dx.doi.org/10.1088/1361-6587/aaacf6.

[26] R. Scannell, M. Beurskens, P. G. Carolan, A. Kirk, M. Walsh, T. O'Gorman, and T. H. Osborne, "Deconvolution of Thomson scattering temperature profiles", *Review of Scientific Instruments*, vol. 82, no. 5, 2011, ISSN: 00346748. DOI: 10.1063/1.3581230.

[27] D. R. Hatch, M. Kotschenreuther, S. M. Mahajan, G. Merlo, A. R. Field, C. Giroud, J. C. Hillesheim, C. F. Maggi, C. Perez Von Thun, C. M. Roach, and S. Saarelma, "Direct gyrokinetic comparison of pedestal transport in JET with carbon and ITER-like walls", *Nuclear Fusion*, vol. 59, no. 8, 2019, ISSN: 17414326. DOI: 10.1088/1741-4326/ab25bd.

[28] T. Lunt, F. Reimold, E. Wolfrum, D. Carralero, Y. Feng, and K. Schmid, "Influence of the first wall material on the particle fuelling in ASDEX Upgrade", *Plasma Physics and Controlled Fusion*, vol. 59, no. 5, p. 55 016, 2017, ISSN: 13616587. DOI: 10.1088/1361-6587/aa659f. [Online]. Available: http://dx.doi.org/10.1088/1361-6587/aa659f.